

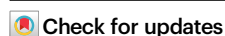


Thermo-responsive chiral micelles as recyclable organocatalyst for asymmetric Rauhut-Currier reaction in water

Received: 16 November 2022

Accepted: 31 October 2023

Published online: 10 November 2023

Lei Xu^{1,2,5}, Li Zhou^{3,5}, Yan-Xiang Li^{3,5}, Run-Tan Gao¹, Zheng Chen¹, Na Liu⁴ & Zong-Quan Wu¹✉

Developing eco-friendly chiral organocatalysts with the combined advantages of homogeneous catalysis and heterogeneous processes is greatly desired. In this work, a family of amphiphilic one-handed helical polyisocyanides bearing phosphine pendants is prepared, which self-assembles into well-defined chiral micelles in water and showed thermo-responsiveness with a cloud point of approximately 38.4 °C. The micelles with abundant phosphine moieties at the interior efficiently catalyze asymmetric cross Rauhut-Currier reaction in water. Various water-insoluble substrates are transferred to target products in high yield with excellent enantioselectivity. The yield and enantiomeric excess (*ee*) of the product generated in water are up to 90% and 96%, respectively. Meanwhile, the yields of the same R-C reaction catalyzed by the polymer itself in organic solvents is <16%, with an *ee* < 72%. The homogeneous reaction of the chiral micelles in water turns to heterogeneous at temperatures higher than the cloud point, and the catalyst precipitation facilitates product isolation and catalyst recovery. The polymer catalyst is recycled 10 times while maintaining activity and enantioselectivity.

One of the important goals in catalysis is the development of eco-friendly catalysts with the combined advantages of homogeneous catalysis and heterogeneous processes, which not only maintain or even improve the catalytic activity and selectivity of homogeneous catalysts but also facilitate product isolation and catalyst recycling^{1–4}. Homogeneous catalysts are widely used in fine-chemical synthesis because typical solid-supported heterogeneous catalysts do not provide the nonpolar environments often required for organic reactions. Soluble polymers are less routinely used catalyst supports that could provide a solvent-like environment for organic reactions^{5–9}. Therefore, polymer skeletons to support catalysts that can increase both catalytic activity and selectivity are greatly desired, especially for chiral catalysts utilized in asymmetric reactions^{10,11}.

Homochirality is one of the most remarkable features of biological molecules¹². Biopolymers can express their homochirality by twisting into one-handed helices (e.g., the α -helix of proteins and the double helix of DNA)^{13,14}. Enzyme-catalyzed stereospecific reactions are believed to arise from the homochirality of macromolecular helix^{15,16}. Inspired by such helices of biomacromolecules, artificial helical polymers have attracted great research attention because of not only their unique structures but also their broad applications, such as chiral recognition and resolution, circularly polarized luminescence, and so forth^{17–30}. Helical polymers are good skeletons to support chiral organocatalysts because helical backbones can provide additional chiral microenvironments, and improve the stereoselectivity of an asymmetric reaction^{31,32}. Helicity itself could

¹State Key Laboratory of Supramolecular Structure and Materials, College of Chemistry, Jilin University, 130012 Changchun, China. ²Key Laboratory of Green and Precise Synthetic Chemistry and Applications, Ministry of Education, Huaibei Normal University, 235000 Huaibei, Anhui, China. ³Department of Polymer Science and Engineering, Hefei University of Technology, 230009 Hefei, China. ⁴The School of Pharmaceutical Sciences, Jilin University, 1266 Fujin Road, 130021 Changchun, Jilin, China. ⁵These authors contributed equally: Lei Xu, Li Zhou, Yan-Xiang Li. ✉ e-mail: zqw@jlu.edu.cn

induce the high enantioselectivity of some asymmetric reactions^{33,34}. Reversing helicity can switch enantioselectivity, thus allowing the obtaining of enantiomeric products^{35,36}. Moreover, the high molecular weight of helical polymers can simplify product isolation and facilitate catalyst recycling, which are particularly desirable for expensive and hardly available chiral catalysts^{10,37–39}. In this respect, polyisocyanide is one of the most attractive helical polymers because of its unique rigid rod-like backbone, high stability, and good self-assembly tendency^{17–21,25}. Therefore, it is a good skeleton for fabricating chiral catalysts for asymmetric reactions.

Water is the cheapest and the most environmentally friendly solvent. As organic compounds are generally nonpolar and water-insoluble, organic reactions in water are commonly restricted⁴⁰. However, enzymes perform catalytic reactions in aqueous systems with high efficiency and excellent selectivity^{41,42}. On the basis of the understanding of enzyme catalysis, polymer-based chiral catalysts have been explored^{43–46}. In contrast, the knowledge about organocatalytic chiral micelles for asymmetric reactions in water with high enantioselectivity and efficiency is still in its infancy. During the past decades, asymmetric organocatalysis has gained great attention because of its advantages, including inexpensive and easily available catalysts, no metal residues, and mild reaction conditions^{47–49}. The Rauhut–Currier (R–C) reaction of two active olefins is a unique and efficient approach for constructing carbon-carbon bonds and densely functionalized organic building blocks^{50–54}. Phosphine-catalyzed intermolecular cross R–C reaction is particularly intriguing among various organocatalyzed reactions⁵². Moreover, because of the poor solubility of reactants and limited catalysts, efficient cross R–C reaction in water with high enantioselectivity has not been realized to date.

We herein describe the construction of chiral organocatalytic micelles using amphiphilic helical polyisocyanide copolymers, composed of hydrophobic helical polyisocyanide bearing phosphine pendants and hydrophilic polyisocyanide carrying methyl triglycol chains. In water, the polymers self-assembled into well-defined chiral micelles with the hydrophobic phosphine pendants at the interior. The micelles catalyzed the asymmetric cross R–C reaction of various water-insoluble substrates in water and yielded the desired products in high yields with excellent enantioselectivity. The enantiomeric excess (ee) and yield of the product were up to 96% and 90%, respectively. Moreover, the block copolymers had excellent thermo-responsiveness in water with a cloud point of 38.4 °C. The precipitation of polymers at temperatures higher than the cloud point facilitated product isolation and catalyst recycling. The polymer catalyst was recycled 10 times with maintained activity and enantioselectivity.

Results

Polymer synthesis and characterization

The block copolymers were prepared following Fig. 1a. Chiral isocyanides (**1r** and **1s**) bearing boron hydride-protected phosphine were polymerized by an alkyne-Pd(II) catalyst and gave the desired polymers in high yield with predicted molar mass (M_n) and low dispersity (M_w/M_n)¹⁷. For example, the M_n and M_w/M_n of poly-**1s**₅₀ (the footnote indicates the initial monomer-to-catalyst feed ratio, as below) were 23.1 kDa and 1.22, respectively, as determined by size exclusion chromatography (SEC) (Fig. 1b). Because polymerization follows a living polymerization mechanism, poly-**1s**₅₀ bearing an active Pd(II)-complex on the chain end was chain extended with achiral isocyanide (**2**) bearing methyl triglycol chains¹⁷. The M_n of the resulting poly(**1s**₅₀-**b-2**₁₀₀) copolymer was

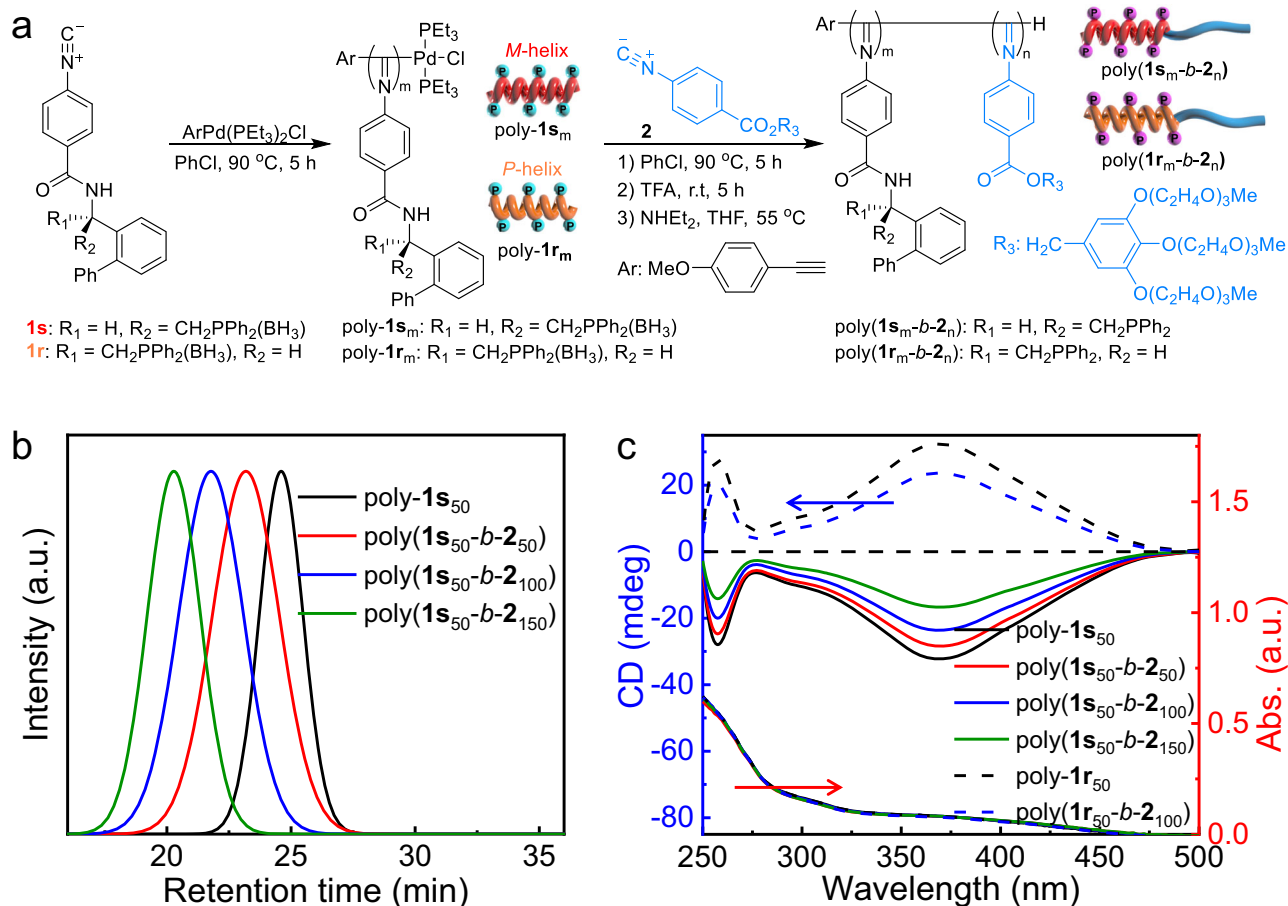


Fig. 1 | **Synthesis of helical polymers.** **a** Synthetic route for polyisocyanide block copolymers. **b** Size-exclusion chromatograms (eluent: THF, the a.u. is the abbreviation of arbitrary units), and **c** CD and UV-vis spectra of the synthetic polymers (0.2 mg/mL, THF, 25 °C).

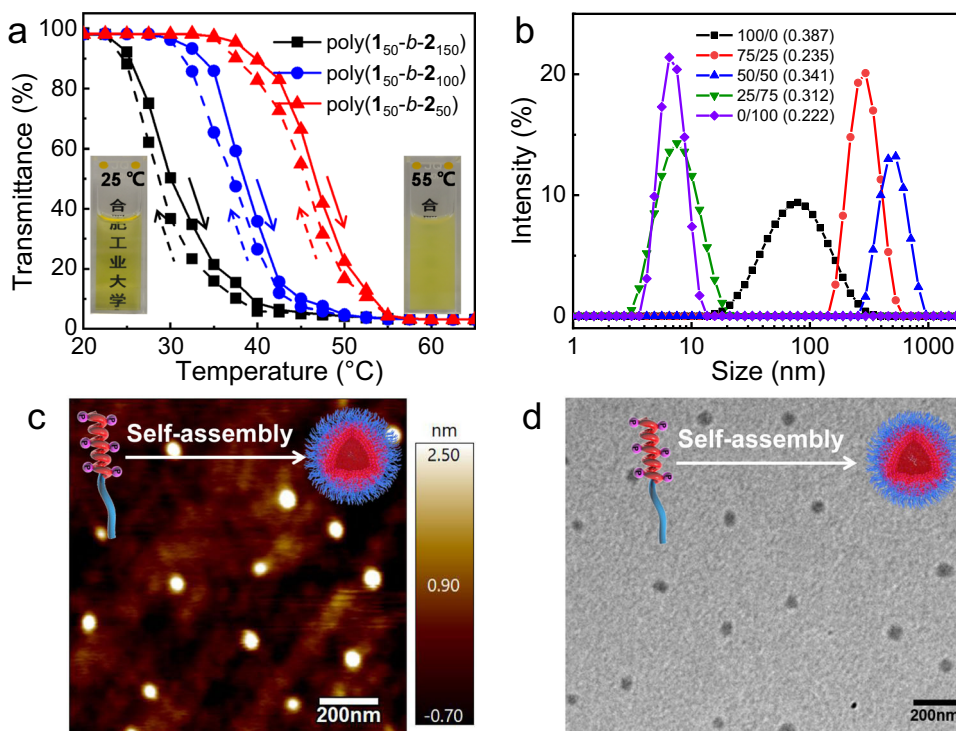


Fig. 2 | Thermo-responsive and self-assembly properties. **a** Plots of the transmittance of poly($\mathbf{1s}_{50}\text{-}b\text{-}\mathbf{2}_{100}$) in water versus temperature (the solid and dashed lines represent the heating and cooling process, respectively). Insets: photographs of poly($\mathbf{1s}_{50}\text{-}b\text{-}\mathbf{2}_{100}$) in H_2O at 25 and 55 °C, 1.0 mg/mL. **b** DLS traces for poly($\mathbf{1s}_{50}\text{-}b\text{-}\mathbf{2}_{100}$) in the mixture of H_2O and THF with different volume ratios (0.2 mg/mL). The

polydispersities for the DLS analyses are 0.387 (H_2O), 0.235 ($\text{H}_2\text{O}/\text{THF} = 75/25$), 0.341 ($\text{H}_2\text{O}/\text{THF} = 50/50$), 0.312 ($\text{H}_2\text{O}/\text{THF} = 25/75$), and 0.222 (THF), respectively. **c** AFM and **d** TEM images of poly($\mathbf{1s}_{50}\text{-}b\text{-}\mathbf{2}_{100}$) casted from the aqueous solution at room temperature.

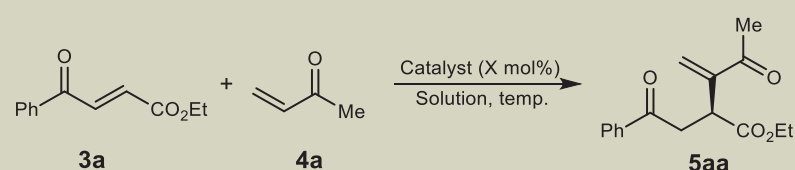
84.2 kDa, and it maintained a low dispersity with $M_w/M_n = 1.25$ (Fig. 1b). The afforded block copolymer was successively treated with triethylphosphine and trifluoroacetic acid to remove the boron hydride that protected the phosphine pendants and the Pd(II)-terminal. Then, poly($\mathbf{1s}_m\text{-}b\text{-}\mathbf{2}_n$) copolymers with different compositions and various block ratios were prepared using the living nature of polymerization (Fig. 1b and Supplementary Table 1). Similarly, poly($\mathbf{1r}_m\text{-}b\text{-}\mathbf{2}_n$) copolymers using enantiomeric $\mathbf{1r}$ instead of $\mathbf{1s}$ were also prepared (Supplementary Table 1). Apart from SEC, these polymers were characterized by ^1H and ^{31}P NMR and FT-IR (Supplementary Figs. 1–9). Because the polymerizations proceeded in a well-controlled living polymerization mechanism, the degree of polymerization was consistent with the initial monomer-to-catalyst feed ratio, according to the detailed studies we reported previously^{11,17,55,56}.

The helicity of the prepared polymers was studied using circular dichroism (CD) spectroscopy in tetrahydrofuran (THF) at 25 °C. Because of the asymmetric induction of the chiral monomer, poly- $\mathbf{1s}_{50}$ showed an intense negative CD in the absorption region of the polyisocyanide backbone, suggesting that the backbone was twisted into a left-handed helix (Fig. 1c)^{55,56}. After chain extension, the resulting poly($\mathbf{1s}_{50}\text{-}b\text{-}\mathbf{2}_n$) showed a negative CD similar to that of the poly- $\mathbf{1s}_{50}$ macroinitiator, whereas the recorded molecular CD intensity was decreased (Fig. 1c). Detailed analyses revealed that the molecular CD intensity of the poly- $\mathbf{1s}_m$ segment was maintained during block copolymerization (Supplementary Fig. 10). The CD decrease was ascribed to $\mathbf{2}$ being achiral, and the resulting poly- $\mathbf{2}_n$ segment could not maintain one-handed helicity; thus, the entire molecular optical activity was decreased. This study confirmed that the poly- $\mathbf{1s}_m$ segment bearing catalytic phosphine pendants of the block copolymers adopted left-handed helicity. The helicity was quite stable, and no obvious change could be detected in various solvents at temperatures from 5 to 60 °C (Supplementary Fig. 11). As anticipated, the poly- $\mathbf{1r}_m$ segment of

poly($\mathbf{1r}_m\text{-}b\text{-}\mathbf{2}_n$) copolymers adopted right-handed helicity, as revealed by CD and adsorption spectroscopy techniques (Fig. 1c and Supplementary Fig. 12)^{55,56}.

Because of their amphiphilic character, the block copolymers could be dissolved in various organic solvents and in water. Interestingly, the transparent aqueous solution of poly($\mathbf{1s}_{50}\text{-}b\text{-}\mathbf{2}_{100}$) turned turbid upon heating and became transparent again after cooling to room temperature, suggesting the turbidimetry-responsiveness with temperature (Fig. 2a). Detailed UV–vis absorption studies revealed that the cloud point was 38.4 °C for poly($\mathbf{1s}_{50}\text{-}b\text{-}\mathbf{2}_{100}$), determined from the temperature corresponding to 50% transmittance of the antisigmoidal transmittance–temperature curve during the heating process⁵⁷. The cloud point decreased with the elongation of poly- $\mathbf{2}_n$ block of the copolymers, it was 46.7, 38.4, and 30.0 °C for poly($\mathbf{1s}_{50}\text{-}b\text{-}\mathbf{2}_{50}$), poly($\mathbf{1s}_{50}\text{-}b\text{-}\mathbf{2}_{100}$), and poly($\mathbf{1s}_{50}\text{-}b\text{-}\mathbf{2}_{150}$), respectively (Fig. 2a).

The self-assembly property of the block copolymers was investigated by adding water to their THF solutions. Dynamic light scattering (DLS) analyses indicated that poly($\mathbf{1s}_{50}\text{-}b\text{-}\mathbf{2}_{100}$) had a hydrodynamic diameter of ca. 8 nm in THF, suggestive of molecular dissolution (Fig. 2b). After adding water, the diameters were 506 and 280 nm for the water contents of 50% and 75%, respectively, suggesting that the amphiphilic block copolymer was self-assembled into micelles with hydrophilic poly- $\mathbf{2}_{100}$ at the exterior and hydrophobic poly- $\mathbf{1s}_{50}$ at the interior. In pure water, the diameter further decreased to 85 nm, indicating that poly($\mathbf{1s}_{50}\text{-}b\text{-}\mathbf{2}_{100}$) was self-assembled into a more compact micelle (Fig. 2b). The critical aggregation concentration (CAC) in water was as low as 0.040 mg/mL, suggesting that this polymer had good self-assembly property (Supplementary Fig. 13). The morphology of the micelles was confirmed by atomic force microscopy (AFM) and transmission electron microscopy (TEM). As displayed in Fig. 2c, the AFM phase image of poly($\mathbf{1s}_{50}\text{-}b\text{-}\mathbf{2}_{100}$) casted from the aqueous solution showed spherical nanoparticles in good homogeneity with a diameter of 75 nm.

Table 1 | Optimization of the R–C reaction condition^a


Run	Catalyst	X ^b	Solution	Temp. (°C)	Yield (%) ^c	ee (%) ^d
1	poly(1s ₅₀ - <i>b</i> - 2 ₁₀₀)	4	CHCl ₃	25	16	70
2	poly(1s ₅₀ - <i>b</i> - 2 ₁₀₀)	4	Toluene	25	14	55
3	poly(1s ₅₀ - <i>b</i> - 2 ₁₀₀)	4	Acetone	25	12	65
4	poly(1s ₅₀ - <i>b</i> - 2 ₁₀₀)	4	EtOH	25	15	50
5	poly(1s ₅₀ - <i>b</i> - 2 ₁₀₀)	4	THF	25	11	72
6	poly(1s ₅₀ - <i>b</i> - 2 ₁₀₀)	4	THF/H ₂ O (75/25)	25	20	75
7	poly(1s ₅₀ - <i>b</i> - 2 ₁₀₀)	4	THF/H ₂ O (50/50)	25	43	80
8	poly(1s ₅₀ - <i>b</i> - 2 ₁₀₀)	4	THF/H ₂ O (25/75)	25	61	84
9	poly(1s ₅₀ - <i>b</i> - 2 ₁₀₀)	4	H ₂ O ^e	25	84	90
10	poly(1s ₅₀ - <i>b</i> - 2 ₅₀)	4	H ₂ O ^e	25	83	79
11	poly(1s ₅₀ - <i>b</i> - 2 ₁₅₀)	4	H ₂ O ^e	25	85	87
12	poly(1s ₅₀ - <i>b</i> - 2 ₁₀₀)	2	H ₂ O ^e	25	56	84
13	poly(1s ₅₀ - <i>b</i> - 2 ₁₀₀)	8	H ₂ O ^e	25	79	81
14	poly(1s ₅₀ - <i>b</i> - 2 ₁₀₀)	10	H ₂ O ^e	25	84	82
15	poly(1s ₅₀ - <i>b</i> - 2 ₁₀₀)	4	H ₂ O ^e	15	83	92
16	poly(1s ₅₀ - <i>b</i> - 2 ₁₀₀)	4	H ₂ O ^e	5	82	94
17	poly(1s ₅₀ - <i>b</i> - 2 ₁₀₀)	4	H ₂ O ^e	0	81	96
18	poly(1r ₅₀ - <i>b</i> - 2 ₁₀₀)	4	H ₂ O ^e	0	82	95 (S)
19	poly- 1s ₅₀	4	H ₂ O ^e	0	51	69
20	1s	4	H ₂ O ^e	0	57	48
21	1r	4	H ₂ O ^e	0	55	49 (S)
22	poly- 1s ₅₀	4	CHCl ₃	0	82	76
23	1s	4	CHCl ₃	0	78	57

^aUnless otherwise specified, all reactions were carried out with **3a** (0.1 mmol) and **4a** (0.3 mmol) in given solvent (5 mL).

^bThe loading of the catalyst was determined by elemental analysis.

^cYield of isolated products.

^dDetermined by HPLC analysis using a chiral column.

^e<5 volume % of THF were used in case the substrates could not be dissolved.

Meanwhile, TEM images further supported that the block copolymer was self-assembled into core-shell-like micelles with a diameter of 72 nm (Fig. 2d). The relatively large size of the micelles was ascribed to the formation of hollowed spherical micelles because of the distinct rigid and rod-like backbone of polyisocyanides^{58,59}. The hollowed micelles might facilitate substrate exchange during the following asymmetric R–C reaction. The cryo-TEM image of poly(**1s**₅₀-*b*-**2**₁₀₀) in water also supported the formation of spherical micelles with a diameter of ca. 90 nm (Supplementary Fig. 14). Other block copolymers showed similar self-assembly properties in water, as revealed by the DLS analyses (Supplementary Fig. 15). Accordingly, poly(**1r**₅₀-*b*-**2**₁₀₀), possessing opposite handed helicity, showed a similar self-assembly behavior (Supplementary Fig. 16).

Asymmetric cross R–C reactions

The catalytic activity of poly(**1s**_m-*b*-**2**_n) micelles for intermolecular cross R–C reactions was explored using ethyl (*E*)-4-oxo-4-phenylbut-2-enoate (**3a**) and but-3-en-2-one (**4a**) as model substrates. Initially, the reaction was conducted at room temperature with 10 mol% catalyst loading of the phosphine pendants of poly(**1s**₅₀-*b*-**2**₁₀₀) in various organic solvents for 48 h. Then, homogeneous reactions occurred and gave the target product **R-5aa**. However, the reaction efficiency was

quite low, and the yields of **R-5aa** were only approximately 16% (runs 1–5, Table 1). The homogeneous cross-R–C reaction in THF and CHCl₃ could give the target product **R-5aa**, but the yield and ee values were not satisfactory (runs 1 and 5, Table 1). The ee of **R-5aa** was generally <72%, as determined by high-performance liquid chromatography (HPLC) using a chiral column (see the Supplementary Information for more details). Then, we conducted the reaction in a mixture of THF and water with different volume ratios. We found that both the reaction rate and enantioselectivity were improved with the addition of water to THF (Fig. 3a and Supplementary Fig. 17). For example, the yields of **R-5aa** were 20%, 43%, and 61% with the addition of 25%, 50%, and 75% water to the THF solution, respectively (runs 6–8, Table 1). In pure water, the isolated yield of **R-5aa** was higher than 84%. The enantioselectivity of the reactions showed the same tendency. As plotted in Fig. 3b, the ee values of the generated **R-5aa** were 75%, 80%, and 84% for the reactions conducted in mixtures of THF and water with 25%, 50%, and 75% water content at room temperature, respectively. As expected, the reaction in water catalyzed by poly(**1s**₅₀-*b*-**2**₁₀₀) showed the best enantioselectivity, the ee of the target was as high as 90%. The polymer catalysts carried chiral carbon centers on the pendants and possessed a chiral helical backbone. Thus, to obtain details on enantioselectivity, asymmetric R–C reaction of **3a** with **4a**

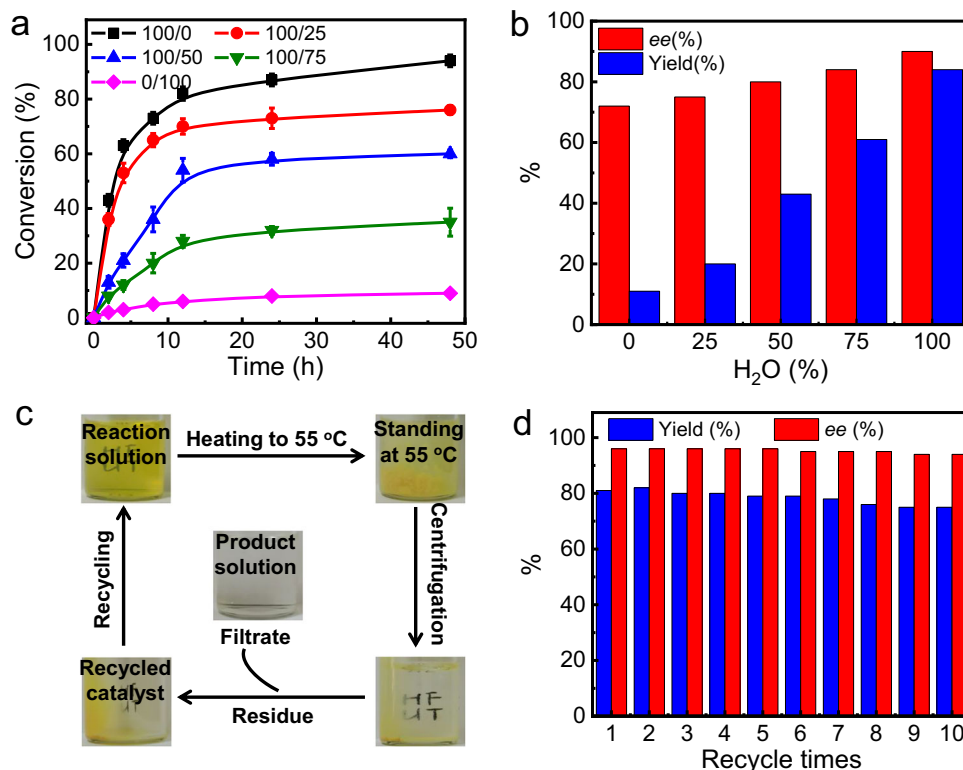


Fig. 3 | Results for the polymer micelle catalyzed cross R-C reaction. **a** Plot of conversion of **3a** versus reaction time catalyzed by poly(**1s**₅₀-*b*-**2**₁₀₀) in different H₂O/THF ratios. Error bars of measured conversion versus reaction time. **b** The

yield and *ee* of **R-5aa** generated in different ratios of H₂O/THF using poly(**1s**₅₀-*b*-**2**₁₀₀) as catalyst. **c** Photographs of the poly(**1s**₅₀-*b*-**2**₁₀₀) catalyst recycling. **d** The results for recycling poly(**1s**₅₀-*b*-**2**₁₀₀) in the reaction of **3a** and **4a**.

catalyzed by the poly-**1s**₅₀ homopolymer, **1r** and **1s** monomers were conducted under identical conditions (runs 19–23, Table 1). The reactions in water gave **5aa** in 51% yield with 69% *ee* using poly-**1s**₅₀ as the catalyst, whereas it gave **5aa** in 57% yield with 48% *ee* using **1s** as the catalyst. The homogeneous reactions in CHCl₃ gave the desired **5aa** in 82% yield and 76% *ee* using poly-**1s**₅₀; and 78% yield and 57% *ee* using **1s**. The **1r** showed behaviors similar to those of **1s** but with opposite enantioselectivity (run 21, Table 1). The relatively higher yield and *ee* values obtained by poly-**1s**₅₀ than those of **1s** confirmed the synergistic effect of the helical backbone and the chiral pendants. In addition, an increase in *M_n* of poly-**1s**_{*n*} could further improve the enantioselectivity of **5aa** until the degree of the polymerization of poly-**1s**_{*n*} reached 50 (Supplementary Fig. 18a). These results indicated the *M_n*-dependent helicity of the poly-**1s**_{*n*} backbone and further supported that the enhanced enantioselectivity came from the helical chirality of the polymer catalyst⁵⁶. Considering the local concentration of substrates within the micelle might influence the catalysis, experiments at different substrate concentrations were performed. The best results were obtained using 0.1 mmol of **3a** with 0.3 mmol of **4a** in water (5 mL) (Supplementary Fig. 18b). A further increase in concentration caused precipitation, whereas the dilution of the substrates gave the product in lower yield. Note that <5% volume of THF was used in case the substrates could not be dissolved in water.

The results inspired us to investigate the effect of catalyst composition on reactions. The cross R-C reaction catalyzed by poly(**1s**₅₀-*b*-**2**₅₀), poly(**1s**₅₀-*b*-**2**₁₀₀), and poly(**1s**₅₀-*b*-**2**₁₅₀) was performed in water under the same conditions. Therein, poly(**1s**₅₀-*b*-**2**₁₀₀) showed the best results in terms of the yield and *ee* of the target product (runs 9–11, Table 1). Thus, this polymer was applied in the following studies. Because poly(**1s**₅₀-*b*-**2**₁₀₀) had good solubility in water, the reaction of **3a** and **4a** was performed in water at 0 °C. As summarized in Table 1, the reaction gave the expected **R-5aa** in 81%

yield and 96% *ee*. Because the CAC of the block copolymer was quite low, the loading of the block polymer catalyst was further decreased to 2 mol% of phosphine pendants; however, both the reaction rate and enantioselectivity decreased considerably (run 12, Table 1). According to these studies, the optimized conditions were carrying the R-C reaction in water at 0 °C with 4 mol% loading of the catalyst (based on the phosphine). Given these results, the intermolecular cross R-C reaction was conducted using the poly(**1r**₅₀-*b*-**2**₁₀₀) catalyst possessing the opposite, right-handed helical backbone under the same conditions described above. Gratifyingly, the reaction of **3a** with **4a** delivered the desired enantiomeric product **S-5aa** in 82% yield and 95% *ee*. These results suggest that the enantioselectivity of the R-C reaction could be reversed by tuning the helicity of the polymer backbone.

The aforementioned results encouraged us to explore the substrate scope of the R-C reaction. Thus, 2-ene-1,4-diones and vinyl ketones with different substituents were prepared and applied in an asymmetric cross-R-C reaction using the poly(**1s**₅₀-*b*-**2**₁₀₀) catalyst. As shown in Table 2, the catalyst was applicable to a wide range of 3-aryl acrylates (**3b–3h**) with different aryl substituents. The targeted products with high yields and excellent enantioselectivities were attained regardless of the electron-donating or electron-withdrawing substituents (runs 1–7, Table 2). Notably, when the ethyl ester group of **3a** was replaced by the less hindered methyl ester (**3i**) or the more hindered isopropyl ester (**3j**) and benzyl ester (**3k**), the desired products (**5ia–5ka**) were also obtained with good yield (82–85%) and excellent enantioselectivity (95–96% *ee*) (runs 8–10, Table 2). Encouraged by these results, the helical polymer-based catalyst was applied to the cross-R-C reaction using aryl-substituted vinyl ketones (**4b–4d**). Gratifyingly, these ketones could also react with various 3-aryl acrylates (**3g** and **3h**) catalyzed by poly(**1s**₅₀-*b*-**2**₁₀₀) in water and gave the expected products in good yields (69–72%) with high *ee* (90–93%)

Table 2 | Scope of the enantioselective R–C reaction catalyzed by poly(1s**₅₀-**b**-**2**₁₀₀)^a**

Run	R ₁ /R ₂ (3)	R ₃ (4)	5	Yield (%) ^b	ee (%) ^c
1	4-F-C ₆ H ₄ /Et (3b)	CH ₃ (4a)	5ba	87	93
2	4-Cl-C ₆ H ₄ /Et (3c)	CH ₃ (4a)	5ca	90	94
3	4-Br-C ₆ H ₄ /Et (3d)	CH ₃ (4a)	5da	86	95
4	4-Me-C ₆ H ₄ /Et (3e)	CH ₃ (4a)	5ea	80	96
5	4-MeO-C ₆ H ₄ /Et (3f)	CH ₃ (4a)	5fa	84	95
6	4-Ph-C ₆ H ₄ /Et (3g)	CH ₃ (4a)	5ga	81	96
7	2-naphthyl/Et (3h)	CH ₃ (4a)	5ha	83	96
8	C ₆ H ₅ /Me (3i)	CH ₃ (4a)	5ia	85	95
9	C ₆ H ₅ /iPr (3j)	CH ₃ (4a)	5ja	83	95
10	C ₆ H ₅ /Bn (3k)	CH ₃ (4a)	5ka	82	96
11	4-Ph-C ₆ H ₄ /Et (3g)	4-Me-C ₆ H ₄ (4b)	5gb	70	92
12	2-naphthyl/Et (3h)	4-Me-C ₆ H ₄ (4b)	5hb	72	90
13	4-Ph-C ₆ H ₄ /Et (3g)	4-F-C ₆ H ₄ (4c)	5gc	69	91
14	2-naphthyl/Et (3h)	4-F-C ₆ H ₄ (4c)	5hc	70	90
15	2-naphthyl/Et (3h)	4-Cl-C ₆ H ₄ (4d)	5hd	71	93
16	2-thienyl/Et (3l)	CH ₃ (4a)	5la	74	88
17	2-Furyl/Et (3m)	CH ₃ (4a)	5ma	76	84
18	tBu/Et (3n)	CH ₃ (4a)	5na	68	89

^aUnless otherwise specified, all reactions were carried out with **3** (0.1 mmol) and **4** (0.3 mmol) in water (5 mL, <5 volume % of THF were used in case the substrates could not be dissolved in water), and the catalyst loading was determined by elemental analysis.

^bYield of isolated products.

^cDetermined by HPLC analysis using a chiral column.

(runs 11–15, Table 2). Furthermore, the substrate scope exploration suggested that poly(**1s**₅₀-**b**-**2**₁₀₀) was also an efficient catalyst for substrates containing heteroaryl groups and aliphatic chains. For example, the reaction of **3l**, **3m**, and **3n** with **4a** gave the expected products **5la**, **5ma**, and **5na** in good yield and high enantioselectivity (runs 16–18, Table 2). Collectively, these studies revealed that the helical polymer is an excellent chiral catalyst for cross-R–C reactions and is applicable to a wide range of substrates.

The amphiphilic poly(**1s**₅₀-**b**-**2**₁₀₀) copolymer had a higher M_n than those of the reactants and products of the R–C reaction and exhibited excellent thermo-responsiveness in water. These characterizations facilitated not only product isolation but also polymer recovery and recycling. Thus, when the R–C reaction of **3a** and **4a** catalyzed by poly(**1s**₅₀-**b**-**2**₁₀₀) in water was accomplished, the aqueous solution was heated to 55 °C, higher than the cloud point of poly(**1s**₅₀-**b**-**2**₁₀₀). The transparent solution immediately turned turbid because of polymer precipitation (Fig. 3c). The precipitated solid was filtrated and washed completely using *n*-hexane to remove the residues of the product and unreacted substrates. The filtrate containing the R–C reaction product was purified and subjected to further analyses. The filter cake of the poly(**1s**₅₀-**b**-**2**₁₀₀) catalyst was reused in the cross-R–C reaction of **3a** and **4a**. To our delight, the recovered catalyst showed high catalytic activity and enantioselectivity. The yield and ee values of the *R*-**5aa** product using the recycled catalyst were almost the same as those generated using the fresh poly(**1s**₅₀-**b**-**2**₁₀₀) catalyst. Poly(**1s**₅₀-**b**-**2**₁₀₀) was recycled 10 times and maintained high activity and enantioselectivity (Fig. 3d). The yield and ee of the product *R*-**5aa** after the 10th reaction were 75% and 94%, respectively.

Discussion

Mechanism study

Because the reactants of the R–C reaction were insoluble in water, the enhanced activity and enantioselectivity of the catalytic block copolymer in water were ascribed to the hydrophobic core of the self-assembled micelles. The amphiphilic block copolymer was self-assembled into spherical micelles in water with hydrophobic and organocatalytic phosphine pendants at the interior and the hydrophilic poly-**2**_n block at the exterior. The water-insoluble reactants were mainly located in the hydrophobic pocket of the micelles. The helical poly-**1s**_m block bearing catalytic phosphine pendants at the interior provided not only catalytic phosphine for the R–C reaction but also a hydrophobic and asymmetric environment for enhancing the enantioselectivity. The asymmetric R–C reaction was catalyzed by the phenyl phosphine pendants. The one-handed helical backbone just provided an additional chiral environment and improved the enantioselectivity^{31–36,56}. Thus, the reaction followed a mechanism similar to that of phenyl phosphine-catalyzed R–C reaction^{50–54}. Moreover, the enriched local concentration of the water-insoluble reactants at the interior accelerated the reaction rate. Collectively, the synergistic effects of the self-assembled micelle facilitated the R–C reaction of water-insoluble materials in water and improved its activity and enantioselectivity. In order to obtain more information, the reaction of **3a** with **4a** catalyzed by poly(**1s**₅₀-**b**-**2**₁₀₀) in water was further monitored using ³¹P NMR spectroscopy. Clearly, there was no interaction between **3a** and poly(**1s**₅₀-**b**-**2**₁₀₀) as no change was observed on the ³¹P NMR spectrum (Supplementary Fig. 19). Meanwhile, an obvious interaction between **4a** and poly(**1s**₅₀-**b**-**2**₁₀₀) was observed because of a new appearance of a ³¹P peak at 33.26 ppm. The Raman analyses also

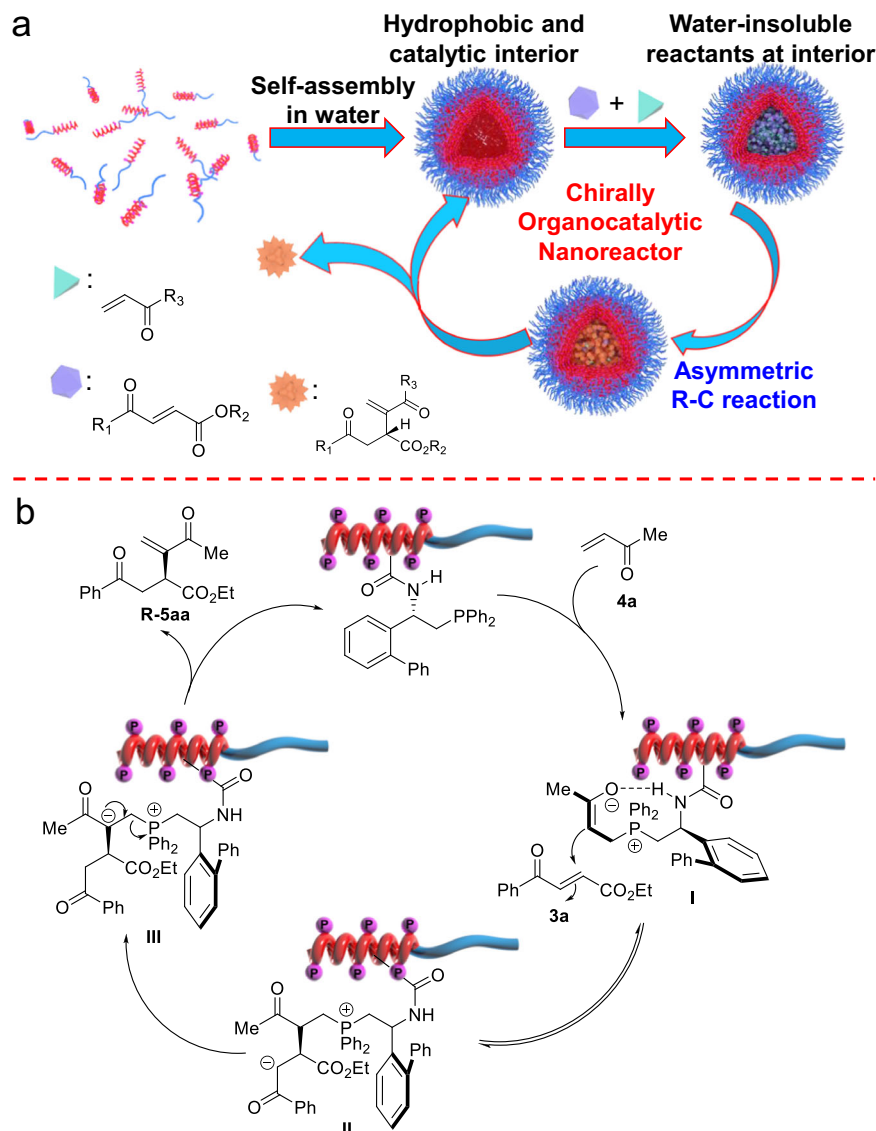


Fig. 4 | Mechanism of the polymer-catalyzed R-C reaction. a Schematic illustration of the helical polymer-micelle catalyzed asymmetric R-C reaction. **b** Possible mechanism for the polymer-catalyzed R-C reaction.

evidenced the intermolecular interaction between poly(**1s**_{50-b-2}**100**) with **4a** in water (Supplementary Fig. 20)²². Based on the above-mentioned results and previous works, we propose a possible mechanism for the reaction^{52–54}. As shown in Fig. 4, the asymmetric cross R-C reaction was initiated by a Michael addition of the phosphine pendant to **4a** and gave an intermediate I. The subsequent nucleophilic addition of I to **3a** yielded intermediate II. Because of the asymmetric environment of the helical backbone, the addition mainly took place from the less steric side of the helix and thus gave intermediate II with high enantioselectivity. Following proton transfer, the final R-C product **R-5aa** and the phosphine catalyst were extruded from intermediate III. Another possible route was the elimination of β -H of intermediate II to obtain the target product. However, based on the work reported by Yu et al., the energy of migration followed by elimination is lower than that for the elimination of β -H in intermediate II⁶⁰. Thus, migration followed by an elimination process is more likely to take place. The amide bonds on the pendants stabilized the one-handed helicity of the polyisocyanide backbone via intramolecular hydrogen bonding^{47,48,55,56}. Moreover, the amide group contributed intramolecular hydrogen bonds and thus stabilized the intermediate I, which enhanced the enantioselectivity of the cross-R-C reaction⁶¹.

To obtain more information about the R-C reaction, we conducted the poly(**1s**_{50-b-2}**100**) catalyzed reaction of deuterium-labeled **3a-d**¹ and **4e-d**² in H₂O, and the reaction of undeuterated **3a** with **4e** in deuterium water D₂O according to above procedure (Fig. 5). The deuterium-labeled experiments gave the desired products with deuterium located at the expected positions. Meanwhile, the reaction conducted in D₂O yielded the same product as that in H₂O. All these studies further confirmed the proposed mechanism.

In summary, we synthesized a family of amphiphilic helical polyisocyanide block copolymers that self-assembled into well-defined chiral micelles in water with catalytic phosphine buried inside the hydrophobic pocket. Such an organocatalytic chiral micelle could efficiently catalyze asymmetric cross R-C reaction of various water-insoluble materials in water and deliver the desired products in high yields with excellent ee values. Here, the ee of the product reached 96% in >81% yields. Moreover, the enantioselectivity could be reversed using helical polyisocyanide copolymers possessing an opposite backbone helicity. The polymer catalysts were applicable to various reactants with just 4 mol% catalyst loading. Moreover, the block copolymers had excellent thermo-responsiveness in water with a cloud point of -38.4 °C. Taking advantage of the thermo-responsiveness and

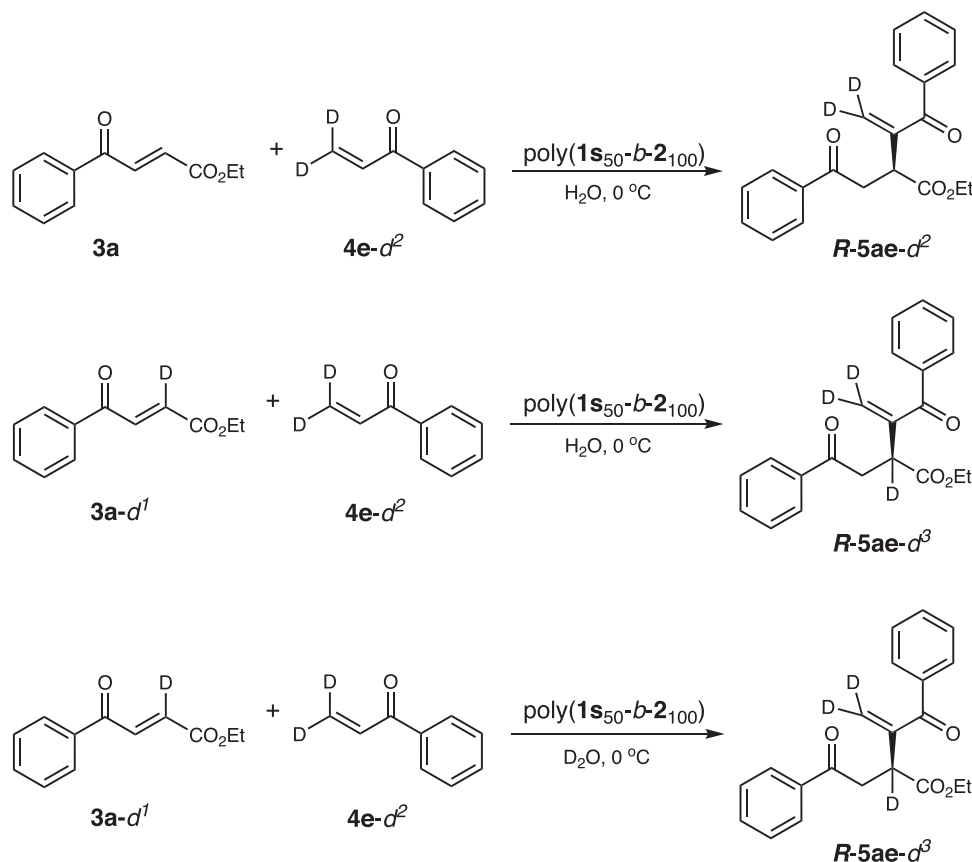


Fig. 5 | Deuterium labeled experiments. Asymmetric cross R–C reactions using **3a** and deuterium labeled **3a-d¹** with deuterium-labeled **4e-d²** in H₂O, and **3a-d¹** with **4e-d²** in deuterated water D₂O at 0 °C with 4% of catalyst loading.

high M_n , the polymer catalyst was recycled 10 times with maintained its high reactivity and enantioselectivity. This study not only provides excellent and environment-friendly catalysts for asymmetric R–C reactions in water but also facilitates the exploration of green catalysts for producing chiral materials.

Data availability

The synthetic details and experimental data generated in this study are all provided in the Supplementary Information. All other data are available from the corresponding author upon request.

References

- Zaera, F. Designing sites in heterogeneous catalysis: are we reaching selectivities competitive with those of homogeneous catalysts? *Chem. Rev.* **122**, 8594–8757 (2022).
- McMorn, P. & Hutchings, G. J. Heterogeneous enantioselective catalysts: strategies for the immobilisation of homogeneous catalysts. *Chem. Soc. Rev.* **33**, 108–122 (2004).
- Zhang, X. et al. Pickering emulsion-derived liquid–solid hybrid catalyst for bridging homogeneous and heterogeneous catalysis. *J. Am. Chem. Soc.* **141**, 5220–5230 (2019).
- Astruc, D., Lu, F. & Aranzas, J. R. Nanoparticles as recyclable catalysts: the frontier between homogeneous and heterogeneous catalysis. *Angew. Chem. Int. Ed.* **44**, 7852–7872 (2005).
- Chi, Y., Scroggins, S.-T. & Fréchet, J. M. J. One-pot multi-component asymmetric cascade reactions catalyzed by soluble star polymers with highly branched non-interpenetrating catalytic cores. *J. Am. Chem. Soc.* **130**, 6322–6323 (2008).
- Bergbreiter, D. E. Soluble polymers as tools in catalysis. *ACS Macro Lett.* **3**, 260–265 (2014).
- Min, H., Miyamura, H., Yasukawa, T. & Kobayashi, S. Heterogeneous Rh and Rh/Ag bimetallic nanoparticle catalysts immobilized on chiral polymers. *Chem. Sci.* **10**, 7619–7626 (2019).
- Dickerson, T. J., Reed, N. N. & Janda, K. D. Soluble polymers as scaffolds for recoverable catalysts and reagents. *Chem. Rev.* **102**, 3325–3344 (2002).
- Altava, B., Burguete, M. I., García-Verdugo, E. & Luis, S. V. Chiral catalysts immobilized on achiral polymers: effect of the polymer support on the performance of the catalyst. *Chem. Soc. Rev.* **47**, 2722–2771 (2018).
- Akai, Y., Yamamoto, T., Nagata, Y., Ohmura, T. & Suginome, M. Enhanced catalyst activity and enantioselectivity with chirality-switchable polymer ligand PQXphos in Pd-catalyzed asymmetric silaborative cleavage of meso-methylenecyclopropanes. *J. Am. Chem. Soc.* **134**, 11092–11095 (2012).
- Song, X., Li, Y.-X., Zhou, L., Liu, N. & Wu, Z.-Q. Controlled synthesis of one-handed helical polymers carrying achiral organoiodine pendants for enantioselective synthesis of quaternary all-carbon stereogenic centers. *Macromolecules* **55**, 4441–4449 (2022).
- Sallembien, Q., Bouteiller, L., Crassous, J. & Raynal, M. Possible chemical and physical scenarios towards biological homochirality. *Chem. Soc. Rev.* **51**, 3436–3476 (2022).
- Yan, X. et al. Single-handed supramolecular double helix of homochiral bis(*N*-amidothiourea) supported by double crossed C–I⋯S halogen bonds. *Nat. Commun.* **10**, 3610 (2019).
- Du, G. et al. Condensed supramolecular helices: the twisted sisters of DNA. *Angew. Chem. Int. Ed.* **61**, e202113279 (2022).
- Kasprzyk-Hordern, B. Pharmacologically active compounds in the environment and their chirality. *Chem. Soc. Rev.* **39**, 4466–4503 (2010).

16. Romanazzi, G., Degennaro, L., Mastrotrilli, P. & Luisi, R. Chiral switchable catalysts for dynamic control of enantioselectivity. *ACS Catal.* **7**, 4100–4114 (2017).
17. Liu, N., Zhou, L. & Wu, Z.-Q. Alkyne-palladium(II)-catalyzed living polymerization of isocyanides: an exploration of diverse structures and functions. *Acc. Chem. Res.* **54**, 3953–3967 (2021).
18. Yashima, E., Maeda, K., Iida, H., Furusho, Y. & Nagai, K. Helical polymers: synthesis, structures, and functions. *Chem. Rev.* **109**, 6102–6211 (2009).
19. Ikai, T. et al. Helix-sense-selective encapsulation of helical poly(lactic acid)s with in a helical cavity of syndiotactic poly(methyl methacrylate) with helicity memory. *J. Am. Chem. Soc.* **142**, 21913–21925 (2020).
20. Xu, L. et al. Crystallization-driven asymmetric helical assembly of conjugated block copolymers and the aggregation induced white-light emission and circularly polarized luminescence. *Angew. Chem. Int. Ed.* **59**, 16675–16682 (2020).
21. Ikai, T., Okubo, M. & Wada, Y. Helical assemblies of one-dimensional supramolecular polymers composed of helical macromolecules: generation of circularly polarized light using an infinitesimal chiral source. *J. Am. Chem. Soc.* **142**, 3254–3261 (2020).
22. Cai, S., Chen, J., Wang, S., Zhang, J. & Wan, X. Allosteric-mimicking self-assembly of helical poly(phenylacetylene) block copolymers and the chirality transfer. *Angew. Chem. Int. Ed.* **60**, 9686–9692 (2021).
23. Chen, J. et al. Polymerization-induced self-assembly of conjugated block copoly(phenylacetylene)s. *Macromolecules* **53**, 1638–1644 (2020).
24. Arias, S., Rodríguez, R., Quiñoá, E., Riguera, R. & Freire, F. Chiral coalition in helical sense enhancement of copolymers: the role of the absolute configuration of comonomers. *J. Am. Chem. Soc.* **140**, 667–674 (2018).
25. Jimaja, S. et al. Nickel-catalyzed coordination polymerization-Induced self-assembly of helical poly(aryl isocyanide)s. *ACS Macro Lett.* **9**, 226–232 (2020).
26. Pfukwa, R., Kouwer, P. H. J., Rowan, A. E. & Klumperman, B. Templated hierarchical self-assembly of poly(*p*-aryltriazole) foldamers. *Angew. Chem. Int. Ed.* **52**, 11040–11044 (2013).
27. Hirose, D., Isobe, A., Quiñoá, E., Freire, F. & Maeda, K. Three-state switchable chiral stationary phase based on helicity control of an optically active poly(phenylacetylene) derivative by using metal cations in the solid state. *J. Am. Chem. Soc.* **141**, 8592–8598 (2019).
28. Yuan, J. & Liu, M. Chiral molecular assemblies from a novel achiral amphiphilic 2-(heptadecyl) naphtha[2,3]imidazole through interfacial coordination. *J. Am. Chem. Soc.* **125**, 5051–5056 (2003).
29. Huang, X. et al. Self-assembled spiral nanoarchitecture and supramolecular chirality in Langmuir–Blodgett films of an achiral amphiphilic barbituric acid. *J. Am. Chem. Soc.* **126**, 1322–1323 (2004).
30. Shen, Z., Jiang, Y., Wang, T. & Liu, M. Symmetry breaking in the supramolecular gels of an achiral gelator exclusively driven by π - π stacking. *J. Am. Chem. Soc.* **137**, 16109–16115 (2015).
31. Ikai, T. et al. Emergence of highly enantioselective catalytic activity in a helical polymer mediated by deracemization of racemic pendants. *J. Am. Chem. Soc.* **143**, 12725–12735 (2021).
32. Yamamoto, T., Murakami, R. & Suginome, M. PQXdppap: helical poly(quininoxaline-2,3-diyl)s bearing 4-(dipropylamino)pyridin-3-yl pendants as chirality-switchable nucleophilic catalysts for the kinetic resolution of secondary alcohols. *Org. Lett.* **23**, 8711–8716 (2021).
33. Yoshinaga, Y., Yamamoto, T. & Suginome, M. Enantioconvergent Cu-catalyzed intramolecular C–C coupling at boron-bound C(sp³) atoms of α -aminoalkylboronates using a C1-symmetrical 2,2'-bipyridyl ligand attached to a helically chiral macromolecular scaffold. *J. Am. Chem. Soc.* **142**, 18317–18323 (2020).
34. Wu, Z.-Q. et al. Achiral organoiodine-functionalized helical polyisocyanides for multiple asymmetric dearomative oxidations. *Nat. Commun.* **14**, 566 (2023).
35. Yamamoto, T., Yamada, T., Nagata, Y. & Suginome, M. High-molecular-weight polyquininoxaline-based helically chiral phosphine (PQXphos) as chirality-switchable, reusable, and highly enantioselective monodentate ligand in catalytic asymmetric hydrosilylation of styrenes. *J. Am. Chem. Soc.* **132**, 7899–7901 (2010).
36. Nagata, Y. et al. Solvent-dependent switch of helical main-chain chirality in sergeants-and-soldiers-type poly(quininoxaline-2,3-diyl)s: effect of the position and structures of the “sergeant” chiral units on the screw-sense induction. *J. Am. Chem. Soc.* **135**, 10104–10113 (2013).
37. Barbaro, P. & Liguori, F. Ion exchange resins: catalyst recovery and recycle. *Chem. Rev.* **109**, 515–529 (2009).
38. Kitanosono, T., Masuda, K., Xu, P. & Kobayashi, S. Catalytic organic reactions in water toward sustainable society. *Chem. Rev.* **118**, 679–746 (2018).
39. Hastings, C. J., Adams, N. P., Bushi, J. & Kolb, S. J. One-pot chemoenzymatic reactions in water enabled by micellar encapsulation. *Green Chem.* **22**, 6187–6193 (2020).
40. García-Fernández, A., Megens, R. P., Villarino, L. & Roelfes, G. DNA-accelerated copper catalysis of Friedel–Crafts conjugate addition/enantioselective protonation reactions in water. *J. Am. Chem. Soc.* **138**, 16308–16314 (2016).
41. Kuepfert, M., Ahmed, E. & Weck, M. Self-assembled thermoresponsive molecular brushes as nanoreactors for asymmetric aldol addition in water. *Macromolecules* **54**, 3845–3853 (2021).
42. Qu, P., Kuepfert, M., Jockusch, S. & Weck, M. Compartmentalized nanoreactors for one-pot redox-driven transformations. *ACS Catal.* **9**, 2701–2706 (2019).
43. Qu, P. et al. Compartmentalisation of molecular catalysts for non-orthogonal tandem catalysis. *Chem. Soc. Rev.* **51**, 57–70 (2022).
44. Soares, B. M. et al. Chiral organocatalysts based on lipopeptide micelles for aldol reactions in water. *Phys. Chem. Chem. Phys.* **19**, 1181–1189 (2017).
45. Rodríguez-Llansola, F., Miravet, J. F. & Escuder, B. A supramolecular hydrogel as a reusable heterogeneous catalyst for the direct aldol reaction. *Chem. Commun.* **47**, 7303–7305 (2009).
46. Lu, A., Cotanda, P., Patterson, J. P., Longbottom, D. A. & O'Reilly, R. K. Aldol reactions catalyzed by L-proline functionalized polymeric nanoreactors in water. *Chem. Commun.* **48**, 9699–9701 (2012).
47. Han, B. et al. Asymmetric organocatalysis: an enabling technology for medicinal chemistry. *Chem. Soc. Rev.* **50**, 1522–1586 (2021).
48. Volla, C. M. R., Atodiresei, I. & Rueping, M. Catalytic C–C bond-forming multi-component cascade or domino reactions: pushing the boundaries of complexity in asymmetric organocatalysis. *Chem. Rev.* **114**, 2390–2431 (2014).
49. Dondoni, A. & Massi, A. Asymmetric organocatalysis: from infancy to adolescence. *Angew. Chem. Int. Ed.* **47**, 4638–4660 (2008).
50. Methot, J. L. & Roush, W. R. Nucleophilic phosphine organocatalysis. *Adv. Synth. Catal.* **346**, 1035–1050 (2004).
51. Xie, P. & Huang, Y. Domino cyclization initiated by cross-Rauhut–Currier reactions. *Eur. J. Org. Chem.* **28**, 6213–6226 (2013).
52. Li, K., Jin, Z., Chan, W.-L. & Lu, Y. Enantioselective construction of bicyclic pyran and hydrindane scaffolds via intramolecular Rauhut–Currier reactions catalyzed by thiourea-phosphines. *ACS Catal.* **8**, 8810–8815 (2018).
53. Dong, X., Liang, L., Li, E. & Huang, Y. Highly enantioselective intermolecular cross Rauhut–Currier reaction catalyzed by a multifunctional Lewis base catalyst. *Angew. Chem. Int. Ed.* **54**, 1621–1624 (2015).
54. Zhou, W. et al. Chiral sulfonamide bisphosphine catalysts: design, synthesis, and application in highly enantioselective intermolecular

- cross-Rauhut–Currier reactions. *Angew. Chem. Int. Ed.* **54**, 14853–14857 (2015).
55. Li, Y.-X. et al. Helicity- and molecular-weight-driven self-sorting and assembly of helical polymers towards two-dimensional smectic architectures and selectively adhesive gels. *Angew. Chem. Int. Ed.* **60**, 7174–7179 (2021).
56. Shen, L., Xu, L., Hou, X.-H., Liu, N. & Wu, Z.-Q. Polymerization amplified stereoselectivity (PASS) of asymmetric Michael addition reaction and aldol reaction catalyzed by helical poly(phenyl isocyanide) bearing secondary amine pendants. *Macromolecules* **51**, 9547–9554 (2018).
57. Cao, G. et al. LCST-type hyperbranched polyoligo(ethylene glycol) with thermo- and CO₂-responsive backbone. *Macromol. Rapid Commun.* **39**, 1700684 (2018).
58. Su, M. et al. Facile synthesis of poly(phenyleneethynylene)-block-polyisocyanide copolymers via two mechanistically distinct, sequential living polymerizations using a single catalyst. *Macromolecules* **49**, 110–119 (2016).
59. Wu, Z.-Q. et al. One-Pot Synthesis of Conjugated Poly(3-hexylthiophene)-b-poly(phenyl isocyanide) Hybrid Rod–Rod Block Copolymers and its Self-Assembling Properties. *J. Polym. Sci., Part A: Polym. Chem.* **51**, 2939–2947 (2013).
60. Xia, Y. et al. An unexpected role of a trace amount of water in catalyzing proton transfer in phosphine-catalyzed (3 + 2). *J. Am. Chem. Soc.* **129**, 3470–3471 (2007).
61. Zhou, W. et al. Enantioselective intermolecular cross Rauhut–Currier reactions of activated alkenes with acrolein. *Chem. Commun.* **52**, 7612–7615 (2016).

Acknowledgements

This work is supported by the Natural Science Foundation of China (NSFC, Nos. 92256201 (Z.-Q.W.), 52273204 (L.Z.), 52273006 (N.L.), 22071041 (Z.-Q.W.), 21971052 (N.L.), 51903072 (L.Z.), and 21871073 (Z.-Q.W.)) and the Fundamental Research Funds for the Central Universities. L. Zhou thanks Anhui Provincial Natural Science Foundation (Grant No. 2008085MB51).

Author contributions

Z.-Q.W., N.L. and L.Z. designed and directed the project; L.X., Y.-X.L., and R.-T.G. performed the experiments and analyzed the data.

Z.-Q.W., N.L. L.Z. and Z.C. wrote the manuscript with input from all other authors.

Competing interests

The authors declare no competing interests.

Additional information

Supplementary information The online version contains supplementary material available at <https://doi.org/10.1038/s41467-023-43092-7>.

Correspondence and requests for materials should be addressed to Zong-Quan Wu.

Peer review information *Nature Communications* thanks Guohua Liu and the other, anonymous, reviewer(s) for their contribution to the peer review of this work. A peer review file is available.

Reprints and permissions information is available at <http://www.nature.com/reprints>

Publisher's note Springer Nature remains neutral with regard to jurisdictional claims in published maps and institutional affiliations.

Open Access This article is licensed under a Creative Commons Attribution 4.0 International License, which permits use, sharing, adaptation, distribution and reproduction in any medium or format, as long as you give appropriate credit to the original author(s) and the source, provide a link to the Creative Commons licence, and indicate if changes were made. The images or other third party material in this article are included in the article's Creative Commons licence, unless indicated otherwise in a credit line to the material. If material is not included in the article's Creative Commons licence and your intended use is not permitted by statutory regulation or exceeds the permitted use, you will need to obtain permission directly from the copyright holder. To view a copy of this licence, visit <http://creativecommons.org/licenses/by/4.0/>.

© The Author(s) 2023